# Bioactive metabolites of edible mushrooms efficacious against androgenic alopecia: Targeting SRD5A2 using computational approach

**Abhay Tiwari**
Centre for Rural Development and Technology, Indian Institute of Technology, New Delhi, Hauz Khas, New Delhi-110016, India https://orcid.org/0000-0001-9408-7917

**Sushil Kumar**
Shaheed Mangal Pandey Govt Girls PG College, Madhavpurum, Meerut-250002, India

**Gourav Choudhir**
Centre for Rural Development and Technology, Indian Institute of Technology, New Delhi, Hauz Khas, New Delhi-110016, India

**Garima Singh**
Centre for Rural Development and Technology, Indian Institute of Technology, New Delhi, Hauz Khas, New Delhi-110016, India

**Upanshu Gangwa**
Department of Chemistry, Indian Institute of Technology, New Delhi, Hauz Khas, New Delhi-110016, India

**Vasudha Sharma**
Department of Food Technology, Jamia Hamdard, New Delhi-110062, India https://orcid.org/0000-0001-8004-5759

**Rupesh K. Srivastava**
Department of Biotechnology, All India Institute of Medical Sciences (AIIMS), New Delhi-110029, India https://orcid.org/0000-0002-3323-0713

**Satyawati Sharma** ( satyawatis@hotmail.com )
Centre for Rural Development and Technology, Indian Institute of Technology, New Delhi, Hauz Khas, New Delhi-110016, India https://orcid.org/0000-0003-0626-9783

---

**Research Article**

**Keywords:** Hair loss, Steroid 5α-reductase2, Mushroom metabolites, Finasteride, Drug likeliness, 5α-dihydroxytestosterone

**Posted Date:** March 17th, 2022

**DOI:** https://doi.org/10.21203/rs.3.rs-1458282/v1

**Version of Record:** A version of this preprint was published at Journal of Herbal Medicine on November 14th, 2022. See the published version at https://doi.org/10.1016/j.hermed.2022.100611.

# Abstract

Introduction

Androgenic alopecia (AGA), the scalp hair loss, occurs due to the hyperactivity of steroid 5α-reductase2 (SRD5A2), which metabolizes testosterone into 5α-dihydroxytestosterone. Finasteride, an FDA-approved drug-producing many side effects, is a commonly used competitive inhibitor for SRD5A2 to treat AGA. As a number of mushrooms species have been used to treat patients having hair loss problems since ancient times, in the present paper, the bioactive metabolites in mushrooms were computationally screened to assess SRD5A2 inhibitory properties and compared with Finasteride.

Methodology

A virtual screening approach in conjunction with molecular dynamics simulation and MMPBSA methods have been applied to identify potential inhibitors against SRD5A2. SwissADME tool and AutoDock Vina were used to screen the library of 156 bioactive mushroom metabolites. All MD simulations were carried out using GROMACS 5.1.4 suite and GROMOS96 43a1 force field. The stability of SRD5A-ligand complexes was determined in terms of RMSD, RMSF, Rg, SASA, and hydrogen bonding. The binding energy of complexes was calculated using MMPBSA.

Results and Conclusion

Virtual screening and MD simulation studies revealed that out of the 156 metabolites, three bioactives, i.e., Zhankuic acid A (-11.5 kcal/mol), Sterenin M (-10.4 kcal/mol), Melleolide K (-10.2 kcal/mol), and drug Finasteride (-4.3 Kcal/mol) having the least binding energy are the potential inhibitors of SRD5A2. These molecules also exhibited stable interaction with SRD5A2 during MD simulation. This study will pave the way for the experimental evaluation and validation of medicinal potentials of screened mushrooms compounds to treat androgenic alopecia.


# Introduction

Androgenic alopecia (AGA) is the most commonly observed hair loss in men and women. This occurs due to the hyperactivity of steroid 5α-reductase2 (SRD5A2) in the hair follicles. The enzyme SRD5A2 is a membrane-bound NADPH-dependent key enzyme in the metabolism of testosterone as it converts testosterone into more active 5α-dihydroxytestosterone (DHT) (Sawaya, 1998; Sinclair, 2004). DHT is the active form of testosterone that binds the androgen receptor in sensitive scalp hair follicles and induces the signaling pathway resulting in miniaturized follicles (Banka et al., 2013). Hyperactivity of SRD5A2 leads to overproduction of DHT and leads to many androgenic ailments such as AGA, benign prostatic hyperplasia (BPH), and prostate cancer (Barratsch et al., 2002). AGA is characterized by the loss of hair in a well-defined pattern that begins above the temples in ‘M’ shape. AGA is not life-threatening but has a significant impact on mental health, self-respect, and overall quality of life (Sinclair 2004).

The steroid 5α-reductases (SRD5As) comprise three isoforms viz. SRD5A1, SRD5A2 and SRD5A3. All the three SRD5As are integral part of endoplasmic reticulum membranes of cells (Scaglione et al., 2017). SRD5A1 iso-enzyme is generally present in sebaceous and sweat glands; SRD5A2 predominates in the skin of genitals, beard, scalp hair follicles, and prostate, while SRD5A3 is found throughout the epidermis and dermis (Godoy et al., 2011). Studies revealed that SRD5A2 is the primary cause of AGA. The cavity inside human SRD5A2 is constructed by seven trans-membrane (TM) domains and six loops. The C-terminal and N-terminal remained towards the cytoplasm and endoplasmic reticulum lumen. A gap present between TM1 and TM2 provides ligand passage to the active site while loop1 (L1) regulates the exchange of NADPH and $NADP^+$ from the cytosol (Khantham et al., 2021). Finasteride and dutasteride are competitive inhibitors for SRD5A2 and only FDA-approved drugs for the treatment of AGA. Both the drugs efficiently inhibit SRD5A2 and treat AGA in due course of medication. The inhibition of SRD5A involves the transfer of hydride ions from NADPH to Finasteride stimulates the formation of an intermediate adduct, NADP- Dihydrofinasteride (NADP-DHF), which inhibits SRD5A by establishing a covalent linkage. Studies indicated that the important amino acid residues in the active site of SDD5A2 include Glu57, Arg114, and Phe118. These residues interact with the intermediate adduct of Finasteride and steroid substrate. Finasteride irreversibly binds with SRD5A2 and significantly reduces the amount of scalp DHT, which improves scalp hair count. Patients treated with Finasteride for about two to four years-maintained hair health up to four years, which progressively reduced in the next three years after drug cessation (Mella et al., 2010). These medications were effective, but they had many adverse effects, especially libido loss and erectile dysfunction (Zhou et al., 2019). Several herbal extracts and their bioactive components from fungi and plants have been used as complementary treatments to stimulate hair development and prevent hair loss (Herman and Herman 2016).

Bioactive metabolites from mushrooms showed a range of health-promoting effects. For healthy hair growth, ancient Mongolians traditionally practiced decoction of *Inonotus obliquus*, the Chaga mushroom (Sagayama et al., 2019). Mushrooms like *Lycoperdon perlatum, Cantharellus cibarius, Lactarius*, and *Coprinus comatus* are delicious and used as medicines for thousands of years. Triterpenoids and some unidentified metabolites exhibited anti-5α-reductase potential extracted from *Ganoderma lucidum* (Fujita et al., 2005; Liu et al., 2006). The present investigation was aimed to explore the anti-5α-reductase2 potential of secondary metabolites from mushrooms using computational approaches. It will open avenues for developing new natural and safe drugs to treat androgenic alopecia.

# Materials And Methods

## 2.1 Metabolite library

A library of 156 secondary metabolites from mushrooms was prepared through a comprehensive literature review for SRD5A2 potential inhibitors identification (Chen and Liu 2017; Tiwari et al., 2022) (Supplementary Table 1). These compounds' structural and chemical attributes, such as molecular formula, IUPAC names, canonical smiles, were retrieved from the PubChem database (Kim et al., 2016).

## 2.2 ADME analysis

SwissADME tool was employed to determine absorption, distribution, metabolism, and excretion for approval of molecules as a drug (Guex and Peitsch 1997). Fifty-eight out of 156 molecules failed because they violated Lipinski's rule of five (Lipinski et al., 1997). Ninety-eight molecules that did not violate the pharmacokinetic and pharmacodynamic properties were further considered for molecular docking.

## 2.3 Protein and ligand preparation

Steroid 5α-reductase2 (PDB ID 7BW1) three-dimensional structure coordinates were fetched from RCSB database (http://www.rcsb.org/pdb/home/home.do). UCSF Chimera was used to remove water and other non-specific molecules (Pettersen et al., 2004). The clean geometry module of discovery studio (San Diego, USA) was utilized to optimize the SRD5A2 structure and saved in the pdb format. Using Molecular Graphics Laboratory (MGL) tool, hydrogen and Kollman charges were added, and the file was saved in pdbqt format.

The ligands that are mushroom's secondary metabolites structures were modified into pdb employing the Open Babel tool by adding explicit hydrogen atoms (O'Boyle et al., 2011). Energy minimization was performed using PyRx's Open Babel tools steepest algorithm, and the structures were saved in pdbqt format (Dallakyan and Olson 2015).

## 2.4 Molecular docking of ligands

For predicting interaction between SRD5A and secondary metabolites from mushrooms was performed employing AutoDock Vina (Trott and Olson 2010). Leaving all other parameters as default, the coordinates X= -30.725, Y = 16.758, and Z = 27.055 were set at the center point grid. The box size was set 22 Å × 22 Å ×22 Å and exhaustiveness at 16. The binding energy of hundred selected molecules fluctuates between − 3.3 to -11.5 kcal/mol. Mushroom metabolites (with binding energy ≥ 10) and drug molecule Finasteride were selected for MD simulation (Molecular Dynamics simulation). The 2D interactions of selected complexes were plotted using the LIGPLOT (Wallace et al., 1996).

## 2.5 Molecular Dynamics simulation

MD simulation is used to comprehend the dynamic motions of each atom. MD was performed for selected mushroom secondary metabolites complexed with SRD5A2 to assess the dynamic properties of these complexes. All simulations were carried out using GROMACS 5.1.4 suite using force field GROMOS96 43a1(Van Der Spoel 2005). The topology files were created employing PRODRG server (Schüttelkopf and Van Aalten 2004). System neutrality was perpetuated by adding an adequate number of ions to the protein complexes; the solvation was carried out in a cubic box of fixed dimensions. The energy minimization was performed using the steepest descent algorithm with convergence criteria lesser than 1000kJ/mol/nm to avoid steric collisions among atoms. PME was used to compute the long-range interactions, and a radius of 9 Å was set for van der Waals and Coulombic interactions (Hess 2008).

Equilibration was executed in two steps. In the first step, solvent and ions were retained unstrained in the NVT ensemble for 100ps; on the other hand, in the second step, restraint weight was bit by bit reduced in the NPT ensemble for 100ps. To maintain all hydrogen bonds constrained LINCS algorithm was used (Hess et al. 1997 Hess; 2008). The trajectory for MD simulation was investigated using Berendsen's temperature and Parrinello-Rahman pressure coupling, which maintained the temperature and pressure at 300 K and 1 atm, respectively (Berendsen et al., 1984). After equilibration, production run was carried out employing LeapFrog dynamics integration. The step size and periodic boundary conditions for timescale were kept at 2 fs and 100 ns.

# 2.6 MMPBSA calculation

Molecular Mechanic-Poisson-Boltzmann surface-area (MMPBSA) was used to ascertain the binding energy shared by each residue. In MMPBSA, the polar fraction of solvation energy (ΔGpsolv) was calculated using the Poisson-Boltzmann equation; and for calculating the non-polar fraction (ΔGnpsolv) the linear relation to the solvent accessible surface area (SASA) was applied. Various fractions of the binding energy of ligand-SRD5A2 complexes were determined employing the g_mmpbsa module of GROMACS (Kumari et al., 2014). The last 10ns of the trajectory were used to analyze binding energy.

# Results And Discussion

### 3.1 Drug likeliness

In silico drug likeliness analysis includes a variety of physicochemical and functional parameters to estimate a molecule's drug-like potential. Physicochemical parameters include size, flexibility, lipophilicity, distribution of electrons, and hydrogen bonding potential. The pharmacophoric parameters comprise absorption, transport, distribution, metabolic stability, affinity to proteins, toxicity, reactivity, etc. influence the interaction of molecules with the living system. In silico screening of molecules based on these characteristics made it easy and least exhaustive to screen a collection of molecules and increase the probability of success in *in-vivo* experiments. Ninety-eight molecules out of 156 molecules of the library exhibited no violation of Lipinski’s rule of five (Supplementary Table 2).

### 3.2 Molecular docking

The binding energy of 98 secondary mushroom metabolites was distributed from -3.3 to -11.5 kcal/mol (Supplementary Table 3). The top molecules exhibiting higher affinities and the least binding energies are Zhankuic acid A (-11.5 kcal/mol), Sterenin M (-10.4 kcal/mol), and Melleolide K (-10.2 kcal/mol), respectively were selected. These mushroom metabolites and Finasteride (approved drug) were preferred for MD simulation (Molecular Dynamics simulation). These molecules form H-bonds and other noncovalent interactions with active site residues of 5α-reductase type2. Zhankuic acid A forms three H-bonds with three different amino acid residues, Arg94, Asn160, and Asp164, with bond lengths of 2.88, 2.91, and 2.98 Å, respectively. Sterenin M was observed to form six hydrogen bonds with five different amino acid residues. Two hydrogen bonds are formed with Tyr107 (bond lengths 2.91 and 2.98

Å). The other four hydrogen bonds between the ligand and amino acid residues with their corresponding bond lengths are Tyr33 (3.04 Å), Leu111 (2.71 Å), Asn193 (3.28Å), and Glu197 (2.75 Å). Melleolide K forms two hydrogen bonds with amino acid residues Tyr33 (3.10 Å) and Arg114 (2.75 Å). The steroidal drug Finasteride forms six hydrogen bonds with five amino acid residues. Two hydrogen bonds are formed between amino acid residue Tyr107 and ligand (2.76 Å and 3.24 Å). Single hydrogen bonds are formed between ligand and amino acid residues Leu20 (2.19 Å), Ala24 (3.05 Å), Tyr98 (2.65 Å), and Arg114 (3.14 Å). (Figure 1). Other noncovalent interactions like van der Waals, ionic, etc., were also observed between ligands and amino acid residues in the substrate-binding pocket of SRD5A2.

### 3.3 Molecular dynamics simulations

MD simulations of selected mushroom metabolites along with the approved drug Finasteride were conducted. The interaction between ligand and protein may cause several conformational disturbances in the 3D structure of the protein. Consequently, to evaluate conformational alterations in protein and stability of SRD5A2-selected mushroom metabolites and Finasteride complexes, we analyzed parameters such as Root-mean-square deviation (RMSD), Root-mean-square fluctuation (RMSF), and Radius of gyration (Rg) for free SRD5A and all SRD5A2-ligand complexes.

#### 3.3.1 Root-mean-square deviation

The RMSD computation of proteins prompts evaluating the level of conformational changes that might happen during MD simulations. To elucidate the stability of SRD5A2 in complexes RMSD of Cα atoms was computed from its starting structures. The RMSD of all systems attained an equilibrium around 20 ns, whereas control (protein) showed some deviation from 45 to 100 ns. The narrow range of variation revealed the stable conformation of the protein in its native and ligand-associated forms. The average RMSD of SRD5A2 backbone and SRD5A2-ligand complexes were ranging ~0.395-0.411nm, whereas the average RMSD of ligands such as compounds Zhankuic acid A (~0.545nm), Sterenin M (~0.632nm), Melleolide K (~0.456nm), and Finasteride (~0.601nm). As the RMSD of all systems was lesser than 0.411nm, it may be assumed that the enzyme's conformation did not change significantly during the course of the simulation. Furthermore, mushroom secondary metabolites association causes no significant conformational changes in the SRD5A backbone (Figure 2).

#### 3.3.2 Root-mean-square fluctuation

RMSF is the measurement of the flexibility of each residue at its average position during simulation. This indicates the dynamics of the system. The RMSF values of SRD5A2 fluctuate in the range of 0.112 to 0.116 nm (Figure 3). The coinciding profile of residue fluctuations demonstrates that the binding of mushroom secondary metabolites and finasteride to the active site does not affect the position of amino acid residues. As a result, it can be concluded that ligand interaction has had no impact on the protein's dynamics.

### 3.3.3 Radius of gyration

The radius of gyration indicates protein compactness, and lower Rg values signify the stability of native and bound proteins. Considering ligand binding might enable a protein to unfold, Rg variation was determined for all cases throughout the course of the simulation. Rg, for the unbound SRD5A2, was centered around ~1.794nm. Similar values (~1.766 to 1.791nm) (Figure 4) were observed for SRD5A2 bound to mushroom secondary metabolites demonstrating that the binding of proposed metabolites causes no change in the integrity and compactness of SRD5A2.

### 3.3.4 Solvent accessible surface area

Hydrophobic interactions between non-polar amino acids increase the stability of globular proteins in solution by protecting non-polar amino acids in hydrophobic cores from the aqueous environment. SASA may theoretically be utilized to detect changes in protein solvent accessibility. It calculates the contribution of each atom in the system's free energy of solvation, such as water, polar and non-polar amino acids. The SASA profile of free SRD5A2 peaked at ~118 $nm^2$, which shifts to ~115-118 $nm^2$ in ligand-protein complexes (Figure 5).

The binding of selected mushroom metabolites does not affect protein folding because the SASA values are less skewed than in control. Table 1 summarizes the mean values of molecular dynamics simulation parameters.

### 3.3.5 Hydrogen bond analysis

The h_bond module of GROMACS was used to calculate the hydrogen bonds formed between SRD5A2 and mushroom metabolites. With the 100 ns simulation, the hydrogen bonds were dispersed, with the maximal hydrogen bonds forming 0.25 to 0.35nm. The graph of hydrogen bonds distribution depicts that it begins at 0.25nm while the distribution was displayed at a distance 0.30 to 0.35nm (Figure 6).

### 3.4 Binding free energy calculation (MMPBSA)

The affinity of the ligand with SRD5A2 was determined employing MMPBSA in terms of binding free energy ($\Delta G_{bind}$) (Table 2). The MMPBSA results indicated that all molecules interact at the active site of SRD5A2 to form stable ligand-protein complexes. Sterenin M showed minimum binding energy and maximum binding affinity among chosen mushroom secondary metabolites, although Finasteride exhibited more binding affinity over mushroom metabolites. $\Delta E_{vdw}$ (energy of *van der* Waals interactions) interaction component and $\Delta G_{psolv}$ free energy and non-polar solvation energy ($\Delta G_{npsolv}$) are the major contributors to the binding free energy of SRD5A2-ligand complexes (Table 2). The mushroom metabolites show higher affinities with SRD5A2 and hence can be the possible inhibitors and efficient lead molecules for the treatment of AGA.

# Conclusion

Virtual screening and MD simulation studies revealed that out of the 156 metabolites, three named Zhankuic acid A, Sterenin M, Melleolide K provide conviction in the articulation of binding energy from molecular docking and MMPBSA. Drug likeliness properties of these molecules unveiled no violation of the Lipinski rule, indicating that the screened metabolites will serve as a strong candidate for drug development against AGA. Findings from the study suggest that the selected mushroom bioactives can be further uptaken for evaluating their drug potential *via in-vitro* and *in-vivo* studies for managing the AGA. Overall, the study proposes edible mushrooms as a potential dietary source towards effective management of AGA, serving as a suitable natural alternate towards commonly used drugs holding adverse side effects on humans.

# Declarations


### Acknowledgment

The authors are grateful to IIT Delhi for providing the high-performance computing facilities for conducting *in-silico* research work.


### CRediT authorship contribution statement

**Abhay Tiwari:** Conceptualization, Library Preparation, Formal analysis, Resources, Data curation, Writing and Editing - original draft **Sushil Kumar:** Writing and Editing draft, Data analysis, Data curation, Proof reading **Gourav Choudhir:** Experimentation, Resources, Analysis, Proof reading **Garima Singh:** Data curation, Visualization, Proof reading **Upanshu Gangwar**: Data curation **Vasudha Sharma and Rupesh K. Srivastava**: Supervision **Satyawati Sharma**: Supervision, Proof-reading, and Resources.

### Declaration of Competing Interest

The authors declare that there is no conflict of interest.

# References


Banka, N., Bunagan, M.J.K., Shapiro, J., 2013. Pattern Hair Loss in Men. Diagnosis and Medical Treatment. Dermatol. Clin. https://doi.org/10.1016/j.det.2012.08.003

Bartsch, G., Rittmaster, R., Klocker, H., 2002. Dihydrotestosterone and the concept of *5alpha-reductase* inhibition in human benign prostatic hyperplasia. World J. Urol. https://doi.org/10.1007/s00345-002-0248-5

Berendsen, H.J.C., Postma, J.P.M., Van Gunsteren, W.F., Dinola, A., Haak, J.R., 1984. Molecular dynamics with coupling to an external bath. J. Chem. Phys. 81, 3684–3690. https://doi.org/10.1063/1.448118

Chen, H.P., Liu, J.K., 2017. Secondary Metabolites from Higher Fungi. Prog. Chem. Org. Nat. Prod. https://doi.org/10.1007/978-3-319-59542-9_1

Dallakyan, S., Olson, A.J., 2015. Small-molecule library screening by docking with PyRx. Methods Mol. Biol. 1263, 243–250. https://doi.org/10.1007/978-1-4939-2269-7_19

Fujita, R., Liu, J., Shimizu, K., Konishi, F., Noda, K., Kumamoto, S., Ueda, C., Tajiri, H., Kaneko, S., Suimi, Y., Kondo, R., 2005. Anti-androgenic activities of *Ganoderma lucidum*. J. Ethnopharmacol. 102, 107–112. https://doi.org/10.1016/j.jep.2005.05.041

Godoy, A., Kawinski, E., Li, Y., Oka, D., Alexiev, B., Azzouni, F., Titus, M.A., Mohler, J.L., 2011. 5α-reductase type 3 expression in human benign and malignant tissues: A comparative analysis during prostate cancer progression. Prostate 71. https://doi.org/10.1002/pros.21318

Guex, N. and Peitsch, M.C., 1997. Swiss PDB Viewer - References. Electrophoresis 18, 2714–2723.

Herman, A., Herman, A.P., 2016. Mechanism of action of herbs and their active constituents used in hair loss treatment. Fitoterapia. https://doi.org/10.1016/j.fitote.2016.08.008

Hess, B., 2008. P-LINCS: A parallel linear constraint solver for molecular simulation. J. Chem. Theory Comput. 4, 116–122. https://doi.org/10.1021/ct700200b

Hess, B., Bekker, H., Berendsen, H.J.C., Fraaije, J.G.E.M., 1997. LINCS: A Linear Constraint Solver for molecular simulations. J. Comput. Chem. 18, 1463–1472. https://doi.org/10.1002/(SICI)1096-987X(199709)18:12<1463::AID-JCC4>3.0.CO;2-H

http://www.rcsb.org/pdb/home/home.do. Last visited on December 20, 2022.

Khantham, C., Yooin, W., Sringarm, K., Sommano, S.R., Jiranusornkul, S., Carmona, F.D., Nimlamool, W., Jantrawut, P., Rachtanapun, P., Ruksiriwanich, W., 2021. Effects on steroid 5-alpha reductase gene expression of thai rice bran extracts and molecular dynamics study on SRD5A2. Biology (Basel). 10. https://doi.org/10.3390/biology10040319

Kim, S., Thiessen, P.A., Bolton, E.E., Chen, J., Fu, G., Gindulyte, A., Han, L., He, J., He, S., Shoemaker, B.A., Wang, J., Yu, B., Zhang, J., Bryant, S.H., 2016. PubChem substance and compound databases. Nucleic Acids Res. 44, D1202–D1213. https://doi.org/10.1093/nar/gkv951

Kumari, R., Kumar, R., Lynn, A., 2014. G-mmpbsa -A GROMACS tool for high-throughput MM-PBSA calculations. J. Chem. Inf. Model. 54, 1951–1962. https://doi.org/10.1021/ci500020m

Lipinski, C.A., Lombardo, F., Dominy, B.W., Feeney, P.J., 2012. Experimental and computational approaches to estimate solubility and permeability in drug discovery and development settings. Adv. Drug Deliv. Rev. https://doi.org/10.1016/j.addr.2012.09.019

Liu, J., Kurashiki, K., Shimizu, K., Kondo, R., 2006. Structure-activity relationship for inhibition of 5α-reductase by triterpenoids isolated from *Ganoderma lucidum*. Bioorganic Med. Chem. 14, 8654–8660. https://doi.org/10.1016/j.bmc.2006.08.018

Mella, J.M., Perret, M.C., Manzotti, M., Catalano, H.N., Guyatt, G., 2010. Efficacy and safety of finasteride therapy for androgenetic alopecia: A systematic review. Arch. Dermatol. https://doi.org/10.1001/archdermatol.2010.256

O'Boyle, N.M., Banck, M., James, C.A., Morley, C., Vandermeersch, T., Hutchison, G.R., 2011. Open Babel: An open chemical toolbox. J. Cheminform. 3, 33. https://doi.org/10.1186/1758-2946-3-33

Pettersen, E.F., Goddard, T.D., Huang, C.C., Couch, G.S., Greenblatt, D.M., Meng, E.C., Ferrin, T.E., 2004. UCSF Chimera–a visualization system for exploratory research and analysis. J. Comput. Chem. 25, 1605–12. https://doi.org/10.1002/jcc.20084

Rathnayake, D., Sinclair, R., 2010. Male androgenetic alopecia. Expert Opin. Pharmacother. https://doi.org/10.1517/14656561003752730

Sagayama, K., Tanaka, N., Fukumoto, T., Kashiwada, Y., 2019. Lanostane-type triterpenes from the sclerotium of *Inonotus obliquus* (Chaga mushrooms) as proproliferative agents on human follicle dermal papilla cells. J. Nat. Med. 73, 597–601. https://doi.org/10.1007/s11418-019-01280-0

Sawaya, M.E., 1998. Novel agents for the treatment of alopecia. Semin. Cutan. Med. Surg. https://doi.org/10.1016/S1085-5629(98)80024-2

Scaglione, A., Montemiglio, L.C., Parisi, G., Asteriti, I.A., Bruni, R., Cerutti, G., Testi, C., Savino, C., Mancia, F., Lavia, P., Vallone, B., 2017. Subcellular localization of the five members of the human steroid 5α-reductase family. Biochim. Open 4, 99–106. https://doi.org/10.1016/j.biopen.2017.03.003

Schüttelkopf, A.W., van Aalten, D.M.F., 2004. PRODRG : a tool for high-throughput crystallography of protein–ligand complexes. Acta Crystallogr. Sect. D Biol. Crystallogr. 60, 1355–1363. https://doi.org/10.1107/S0907444904011679

Trott, O., Olson, A.J., 2009. AutoDock Vina: Improving the speed and accuracy of docking with a new scoring function, efficient optimization, and multithreading. J. Comput. Chem. 31, NA-NA. https://doi.org/10.1002/jcc.21334

Van Der Spoel, D., Lindahl, E., Hess, B., Groenhof, G., Mark, A.E., Berendsen, H.J.C., 2005. GROMACS: Fast, flexible, and free. J. Comput. Chem. https://doi.org/10.1002/jcc.20291

Wallace, A.C., Laskowski, R.A., Thornton, J.M., 1995. Ligplot: A program to generate schematic diagrams of protein-ligand interactions. Protein Eng. Des. Sel. 8, 127–134. https://doi.org/10.1093/protein/8.2.127

Zhou, Z., Song, S., Gao, Z., Wu, J., Ma, J., Cui, Y., 2019. The efficacy and safety of dutasteride compared with finasteride in treating men with androgenetic alopecia: A systematic review and meta-analysis. Clin. Interv. Aging. https://doi.org/10.2147/CIA.S192435

# Tables

**Table 1**: Average values of bioactives for different parameters of molecular dynamics simulation

| Parameter | Control | Zhankuic acid A | Sterenin M | Melleolide K | Finasteride |
|---|---|---|---|---|---|
| **Backbone RMSD** | 0.502 ± 0.069 | 0.403 ± 0.024 | 0.402 ± 0.022 | 0.410 ± 0.033 | 0.395 ± 0.032 |
| **Complex RMSD** | | 0.410 ± 0.023 | 0.407 ± 0.023 | 0.411±0.033 | 0.405 ± 0.031 |
| **Ligand RMSD** | | 0.545 ± 0.063 | 0.632 ± 0.075 | 0.456 ± 0.031 | 0.601 ± 0.039 |
| **RMSF** | 0.165 ± 0.064 | 0.116 ± 0.051 | 0.112 ± 0.041 | 0.114 ± 0.049 | 0.112 ± 0.063 |
| **Rg** | 1.794 ± 0.016 | 1.791 ± 0.009 | 1.791 ± 0.011 | 1.766 ± 0.013 | 1.788 ± 0.013 |
| **SASA** | 118.933 ± 3.322 | 117.329 ± 2.780 | 118.210 ± 2.908 | 116.748 ± 3.828 | 115.412 ± 2.917 |

RMSD: Root-mean-square deviation; SASA: solvent accessible surface area; RMSF: Root-mean-square fluctuation; Rg: Radius of gyration

**Table 2:** Binding free energy of mushroom metabolites

| Ligand | Van der Waals energy (kJ/mol) | Electrostatic energy(kJ/mol) | Polar solvation energy (kJ/mol) | SASA energy (kJ/mol) | Binding energy (kJ/mol) |
|---|---|---|---|---|---|
| Zhankuic acid A | -287.840 ± 10.477 | -80.311 ± 9.587 | 173.341 ± 15.998 | -21.895 ± 1.125 | -216.705 ± 15.250 |
| Sterenin M | -314.367 ± 12.287 | -39.684 ± 9.823 | 107.576 ± 9.445 | -22.667 ± 1.093 | -269.142 ± 13.985 |
| Melleolide K | -265.022 ± 13.032 | -23.453 ± 7.694 | 89.916 ± 9.358 | -19.686 ± 0.906 | -218.245 ± 13.063 |
| Finasteride | -607.836 ± 17.561 | -34.501 ± 8.473 | 197.942 ± 16.297 | -41.314 ± 1.206 | -485.709 ± 21.331 |

SASA: solvent accessible surface area

# Figures

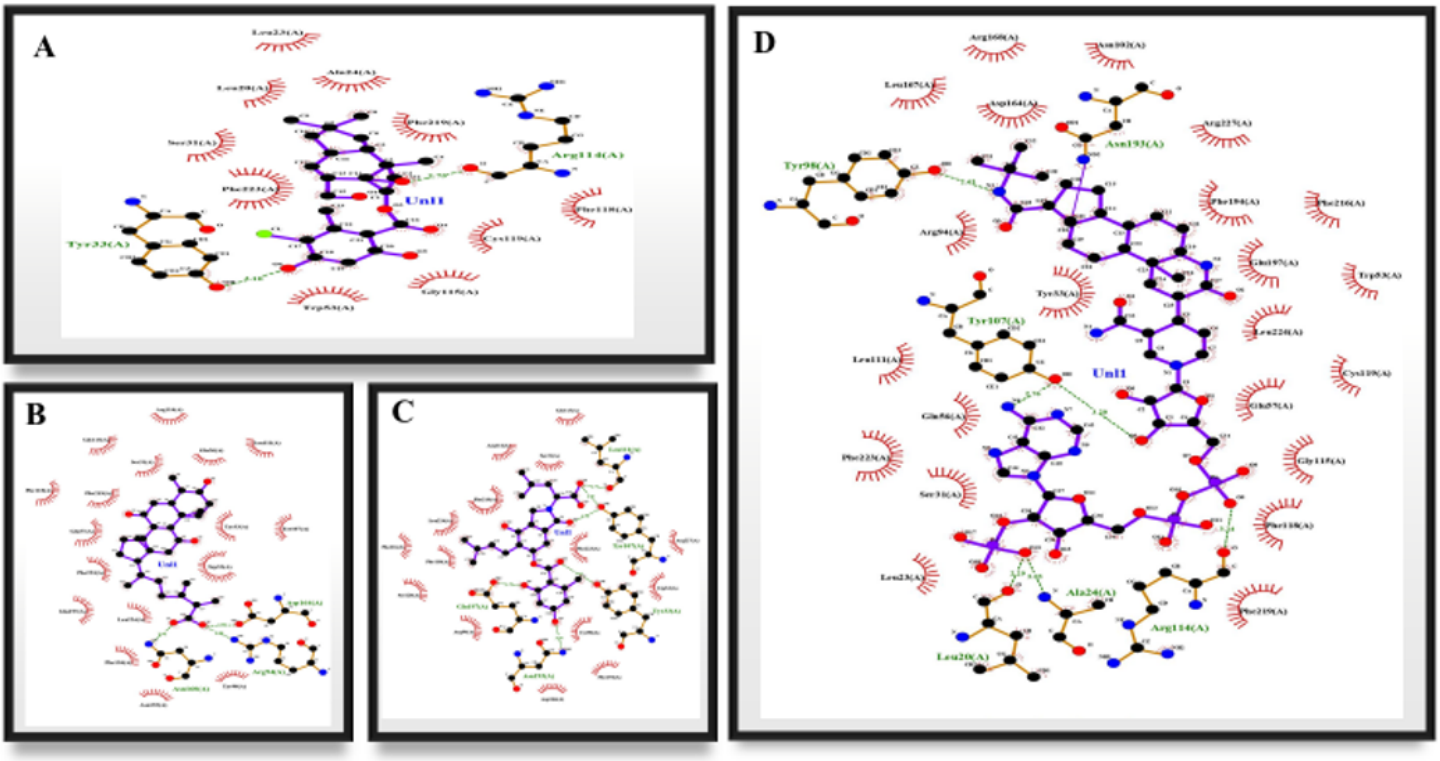


Figure 1

Molecular Docking Interactions of (A) Melleolide K, (B) Zhankuic acid A, (C) Sterenin M, (D) Co-crystalized ligand with SRD5A2

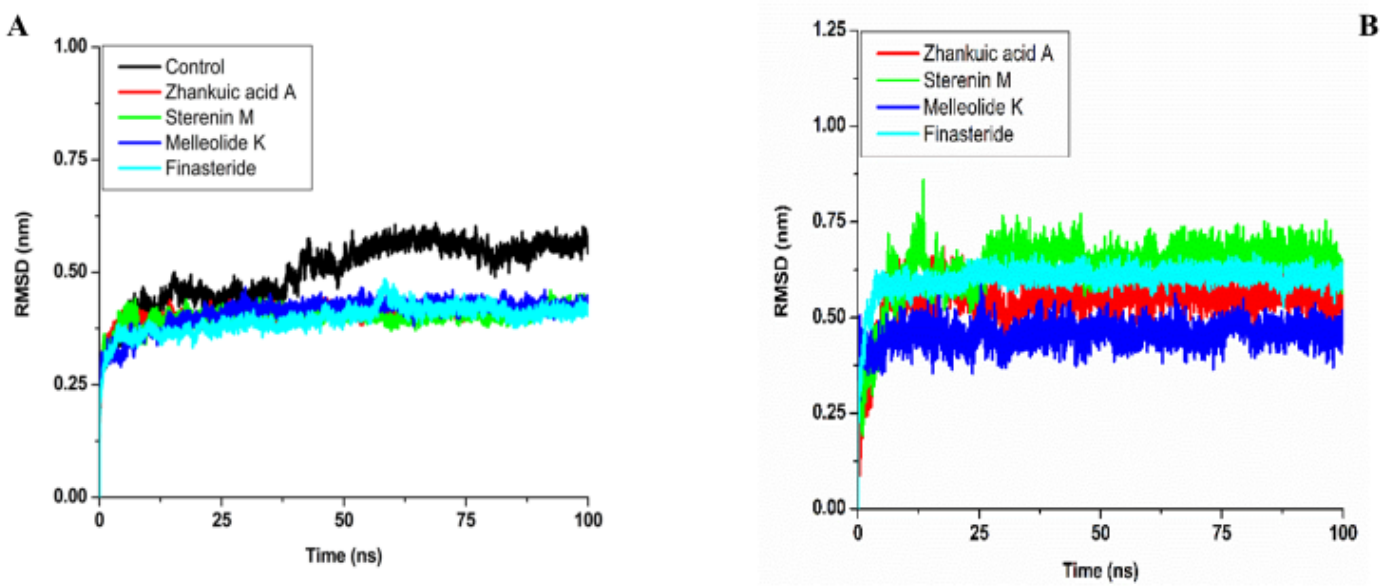


## Figure 2

RMSD profile of SRD5A2 backbone atoms (A) in control and ligand-bound states (B) RMSD of individual ligands during the simulation

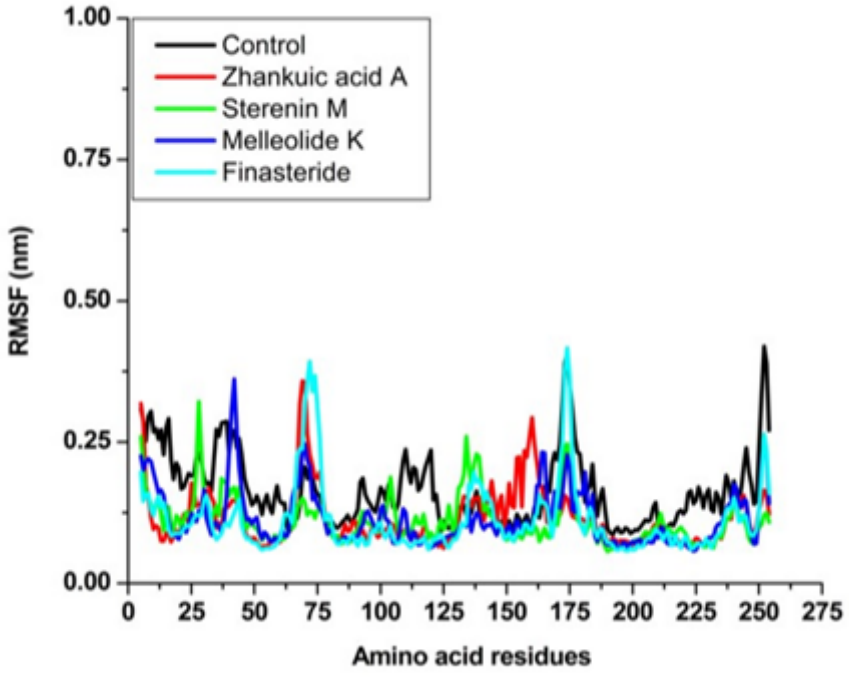

## Figure 3

RMSF of SRD5A2 in unbound as well as in ligand-bound states

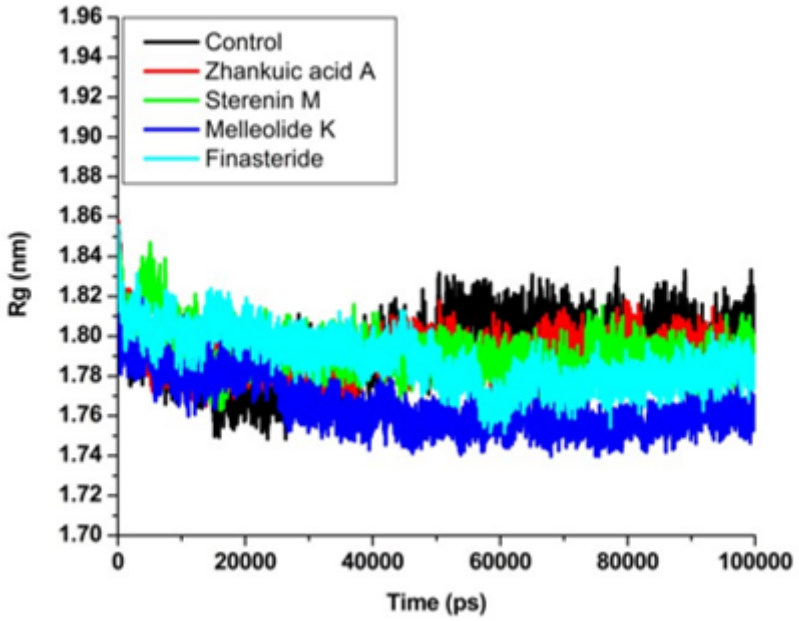


## Figure 4

Variation in Radius of Gyration (Rg) of SRD5A2 complex with proposed inhibitors

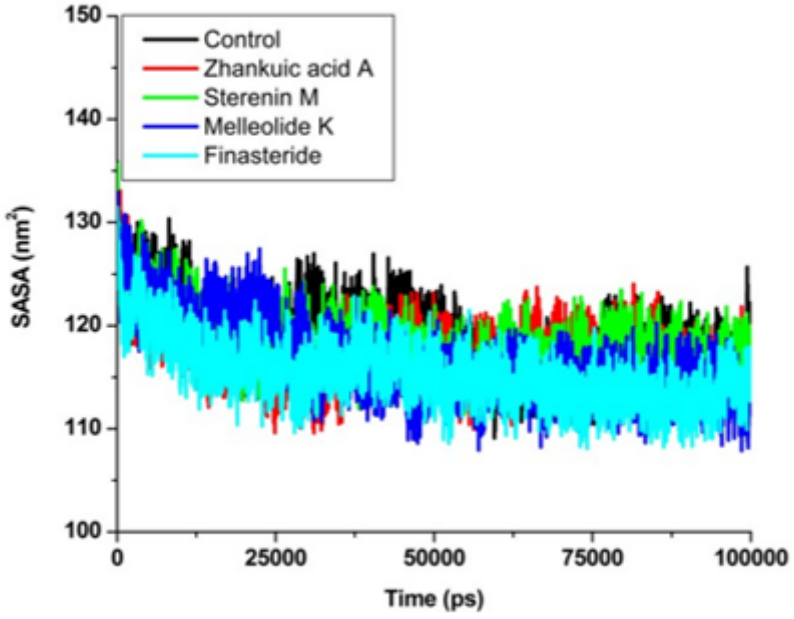

**Figure 5**

Variation of the SASA of SRD5A2 complex with secondary mushroom metabolites during the course of the simulation

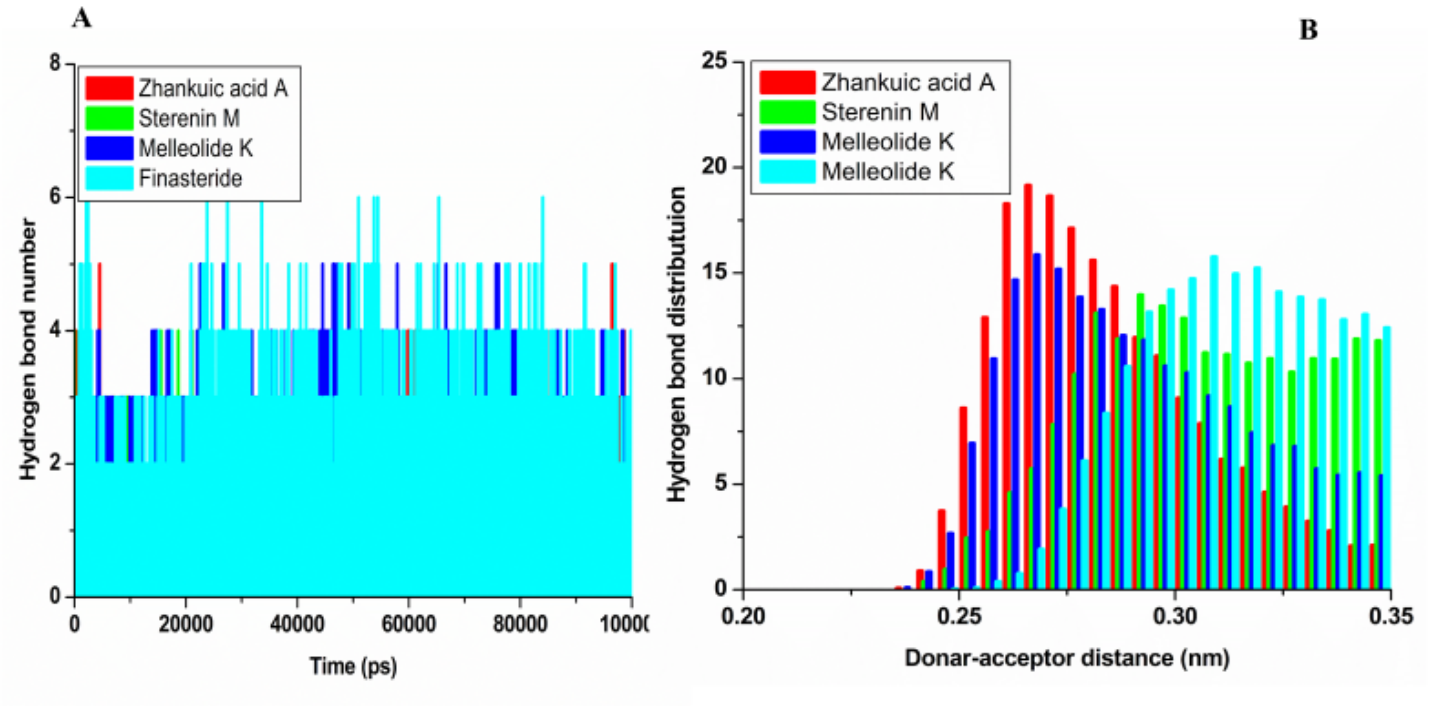


**Figure 6**

Hydrogen bond number (A) and distribution (B) between selected bioactive mushroom metabolites and SRD5A2.

# Supplementary Files

This is a list of supplementary files associated with this preprint. Click to download.

- SupplementaryTable1.pdf
- SupplementaryTable2.xlsx
- supplymentarytable3.pdf